Effects of Interaction and Disorder for Dirac Fermions in 2D Graphene: IQHE, Phase Diagram and Pseudo-Spin Ferromagnet

Donna Sheng (Cal. State Univ. Northridge)

In collaboration with:

L. Sheng (UH), Z. Y. Weng (Tsinghua Univ. China)

F. D. M. Haldane (Princeton) and L. Balents (UCSB)

NSF, PRF and DOE support

Outline:

IQHE in honeycomb lattice model with disorder: Topology, phase diagram, and Anderson localization (noninteracting case). Delocalization or antilocalization at B=0 near the Dirac point

Effect of interaction: pseudospin state, and odd integer QHE states for interaction electrons in graphene: comparison of mobility gap at $\nu=1$ and $\nu=3$

Effect of spin-orbit coupling, QSHE

numerical calculations of IQHE for honeycomb lattice model with random disorders

Experimental observation of the "half-integer" quantized IQHE: (-3/2, -1/2, 1/2, 3/2)* 4e^2/h

Theoretical work using continuous model for Dirac fermions can account/predicted such quantizations:
Gusynin et al. Peres et al.
Zheng and Ando

Curious about what is happening in the whole energy region of the band for electrons in honeycomb lattice model

K. S. Novoselov et al., Nature (2005)

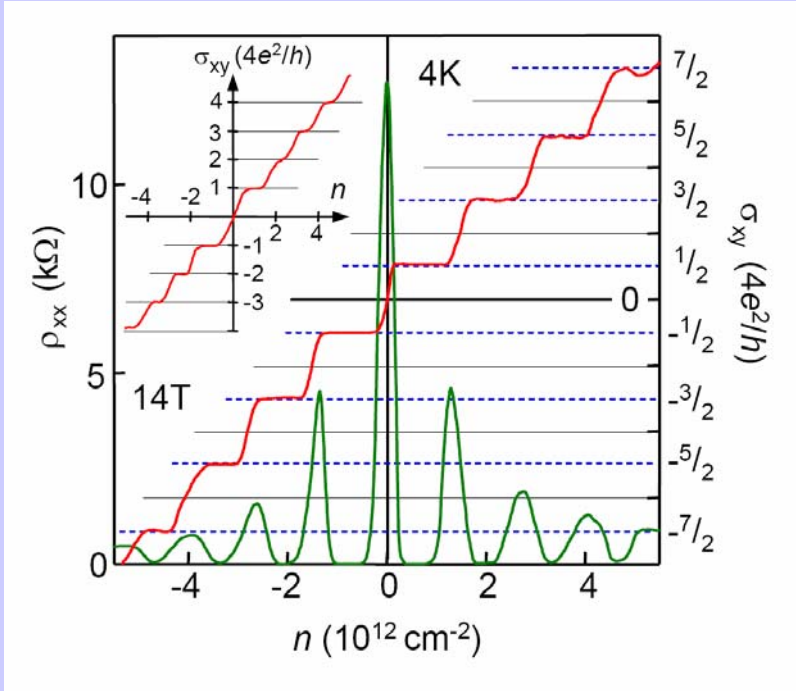

Three regions of IQHE in the energy band
IQHE for Dirac fermions in the middle

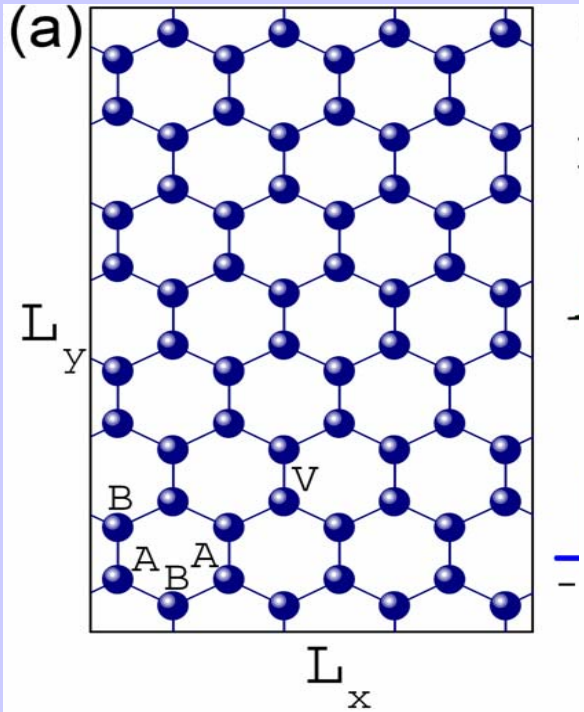

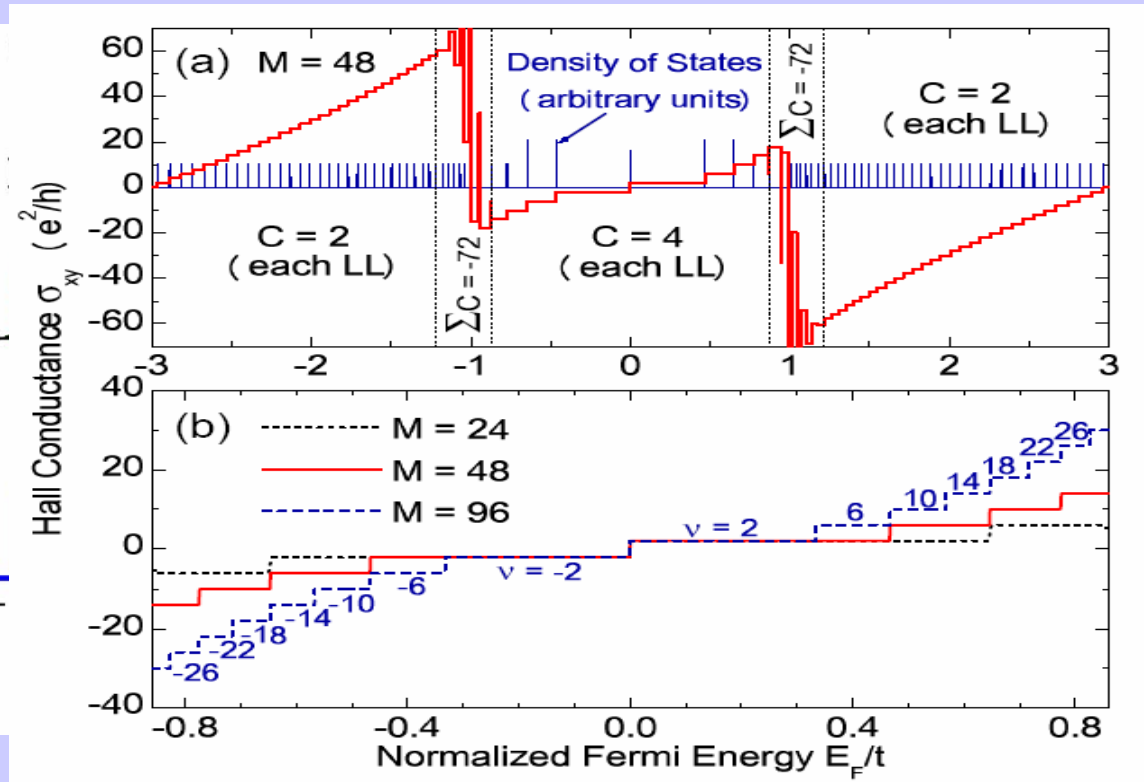

$$H = -t\sum C_{iB}^{+} C_{jA} e^{iA_{ij}} + h.c + \sum w_i C_i^{+} C_i$$

$\Phi = 2\pi/M$

Effect of disorder and phase diagram: PRB 73 (2006)

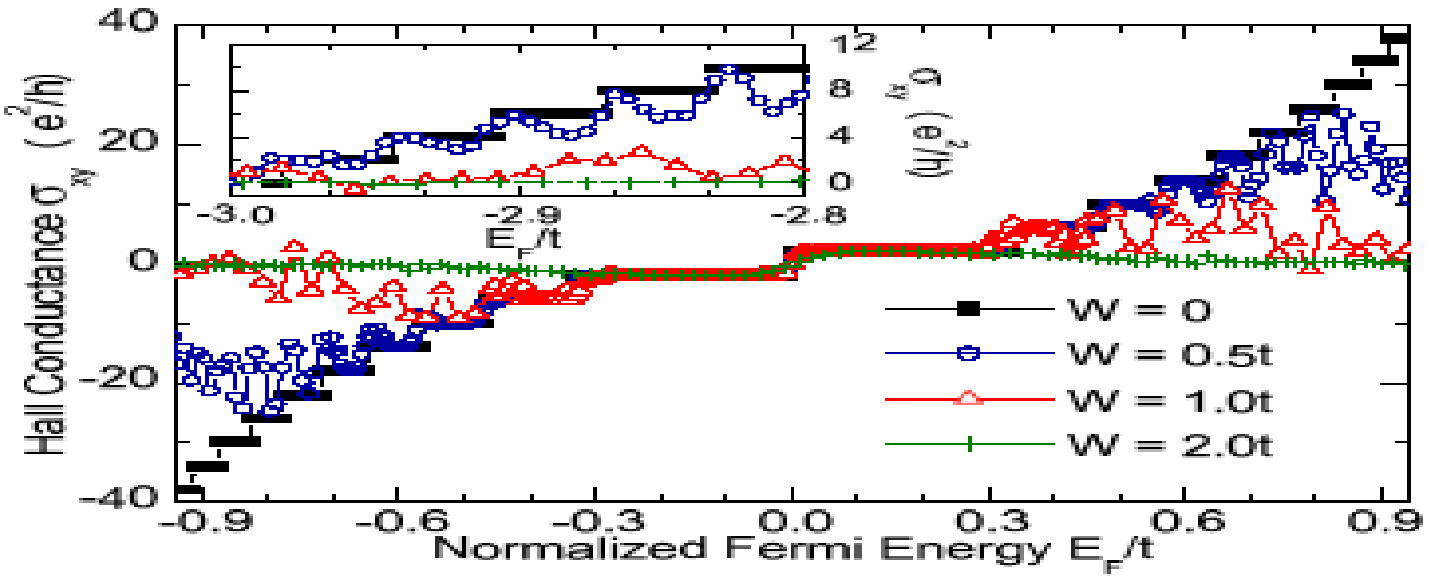

FIG. 2: Unconventional Hall conductance as a function of electron Fermi energy near the band center for four different disorder strengths each averaged over 200 disorder configurations. Inset: conventional Hall conductance near the lower band edge. Here $M = 96$ and the sample size is 96×48.

Phase diagram

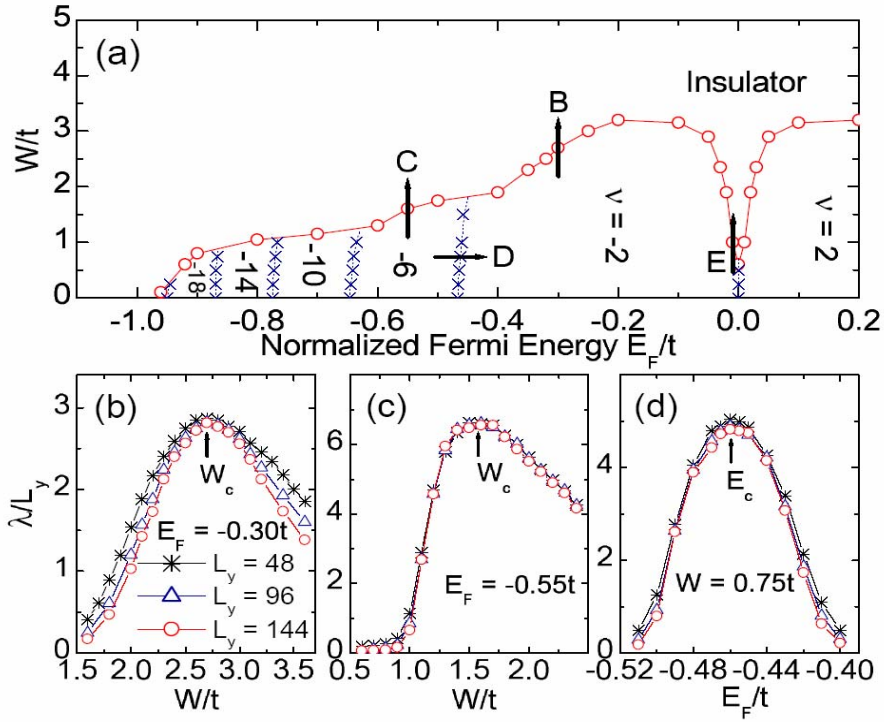

Disorder splits the extended level at the center of n=0 LL, leaving n=0 region an insulating phase

FIG. 3: (a) Phase diagram for the unconventional QHE regime in graphene at $M = 48$, which is symmetric about $E_F = 0$. (b) to (d): Normalized localization lengths calculated for three bar widths $L_y = 48$, 96 and 144, as the phase boundary is crossed by the paths indicated by the arrows B, C and D in (a), respectively.

Experiment discovers ν=1 IQHE and "ν=0" insulating phase

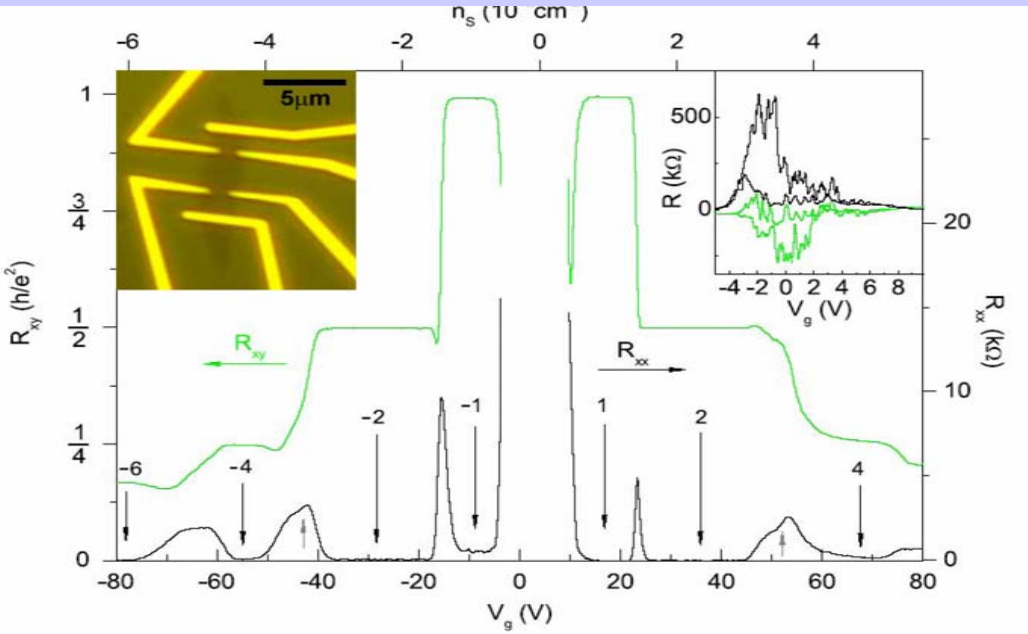

Y. Zhang et. al., PRL 2006

FIG 1. (color online) R_{xx} and R_{xy} measured in the device shown in the left inset, as a function of V_g at $B = 45$ T and $T = 1.4$ K. $-R_{xy}$ is plotted for $V_g > 0$. The numbers with the vertical arrows indicate the corresponding filling factor ν. Gray arrows indicate developing QH states at $\nu = \pm 3$. n_s is the sheet carrier density derived from the geometrical consideration. Right inset: R_{xx} (dark solid lines) and R_{xy} (light solid lines) for another device measured at $B = 30$ T and $T = 1.4$ K in the region close to the Dirac point. Two sets of R_{xx} and R_{xy} are taken at different time under the same condition. Left inset: an optical microscope image of a graphene device used in this experiment.

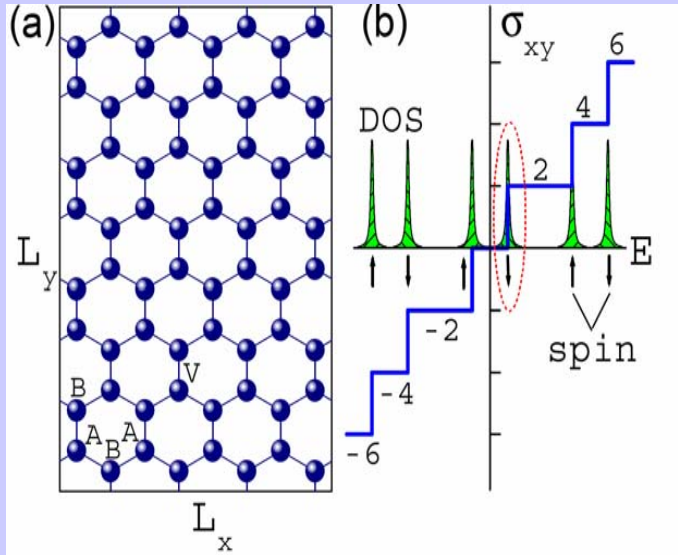

Interaction has to be taken into account to explain the ν=1IQHE---Pseudospin Ferromagnet?

delocalization of Dirac fermions at B=0 (a different issue)

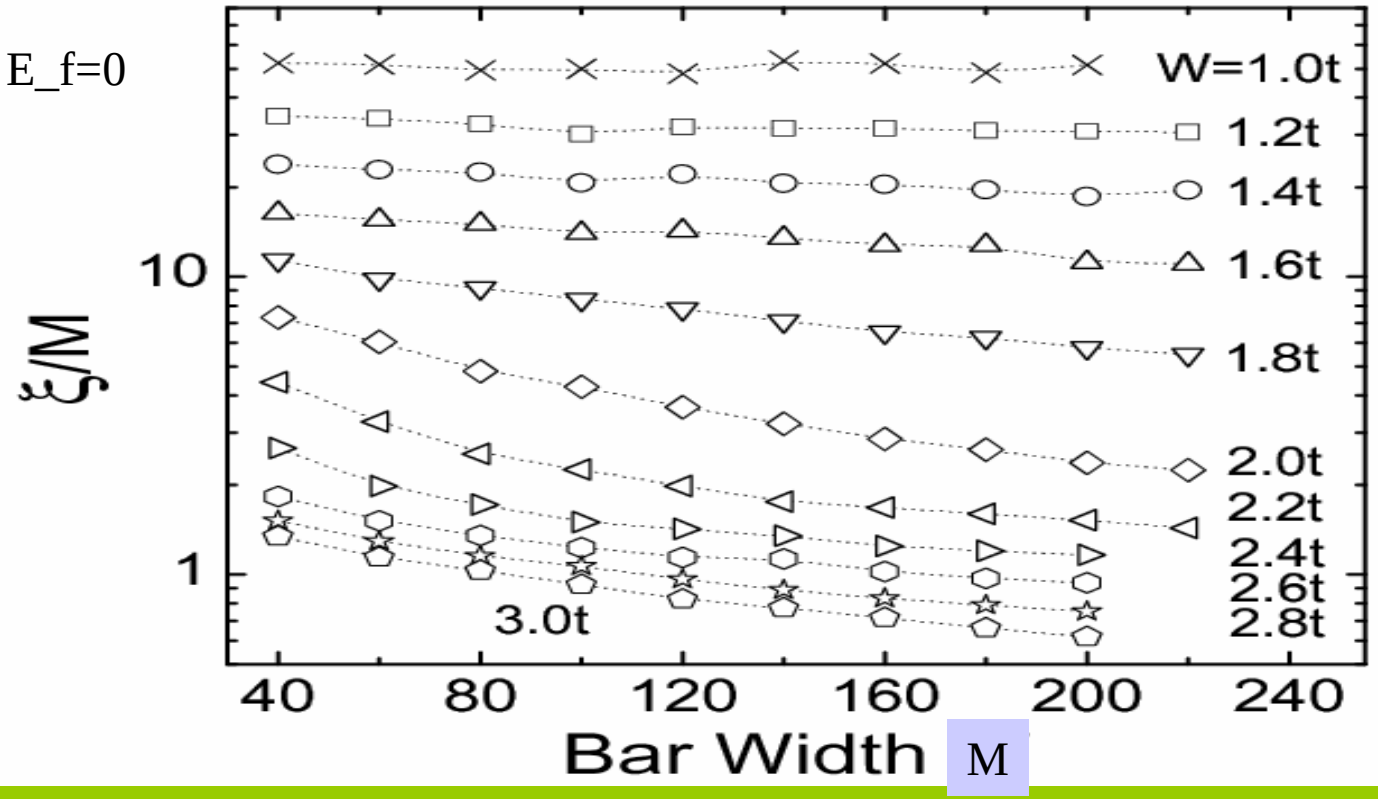

Transfer matrix calculation of the “finite size localization length” for quasi-1D system with width M, it indicates “delocalization” at Dirac point E_f=0 at W<1.0t, or “exponential large” localization length at thermodynamic limit

Experiment discovers ν=1 IQHE and "ν=0" insulating phase

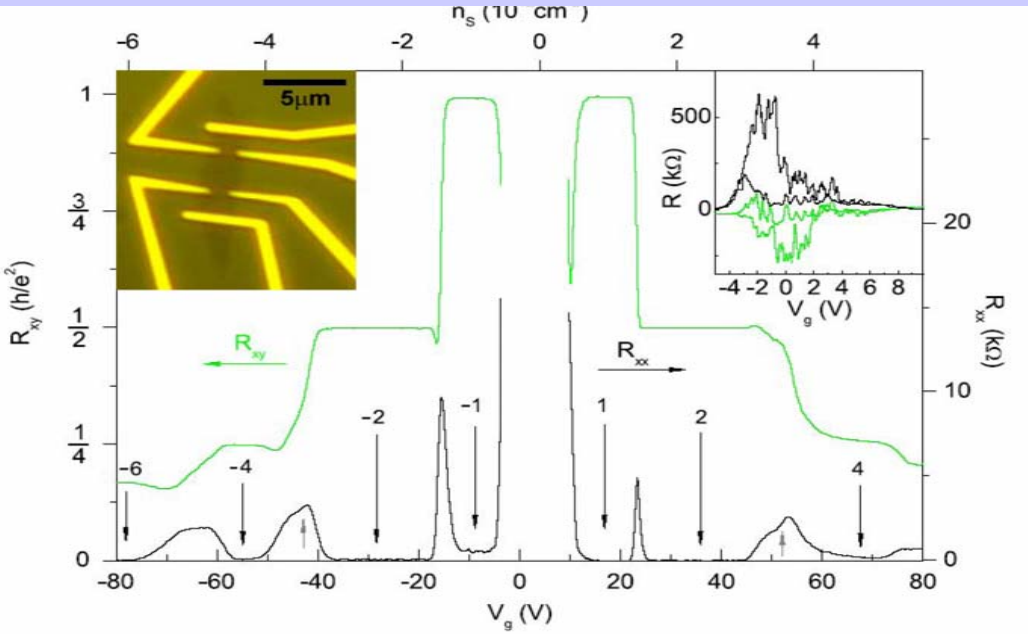

Y. Zhang et. al., PRL 2006

FIG 1. (color online) R_{xx} and R_{xy} measured in the device shown in the left inset, as a function of V_g at $B = 45$ T and $T = 1.4$ K. $-R_{xy}$ is plotted for $V_g > 0$. The numbers with the vertical arrows indicate the corresponding filling factor ν. Gray arrows indicate developing QH states at $\nu = \pm 3$. n_s is the sheet carrier density derived from the geometrical consideration. Right inset: R_{xx} (dark solid lines) and R_{xy} (light solid lines) for another device measured at $B = 30$ T and $T = 1.4$ K in the region close to the Dirac point. Two sets of R_{xx} and R_{xy} are taken at different time under the same condition. Left inset: an optical microscope image of a graphene device used in this experiment.

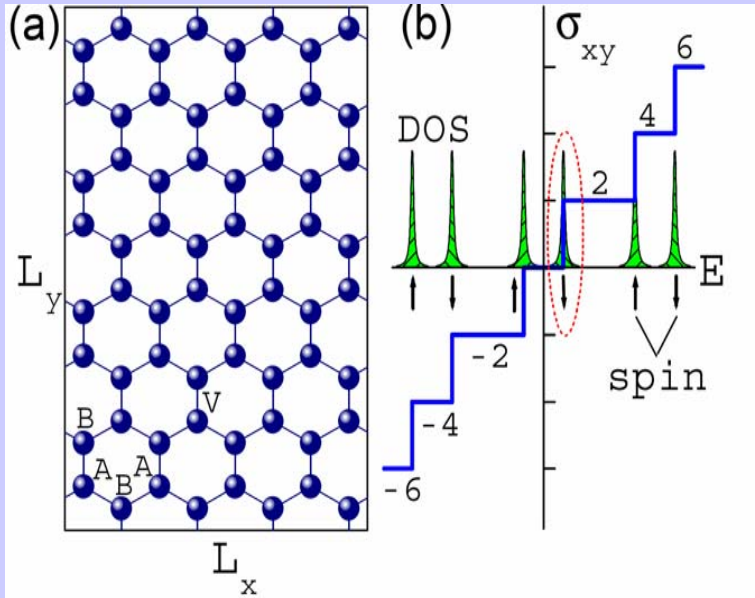

Interaction has to be taken into account to explain the ν=1 IQHE---Pseudospin Ferromagnet?

Interaction and disorder effects: finite size exact diagonalization

- Theoretical (more analytical) works

Nomura & MacDonald

Alicea & Fisher

Yang et al.

Gusynin et al.

Toke & Jain

Goerbig et al.

Haldane's Pseudo-Potential gives rise to incompressible state, SU(4) invariant, Algebraic correction (a/l) to SU(4) may also be important

When use C_A, C_B as slow varying Dirac particles, Coulomb interaction cannot be strictly written as terms only involving: V_ij n_i n_j (Alicea et al. and Goerbig et al.)

Lattice model

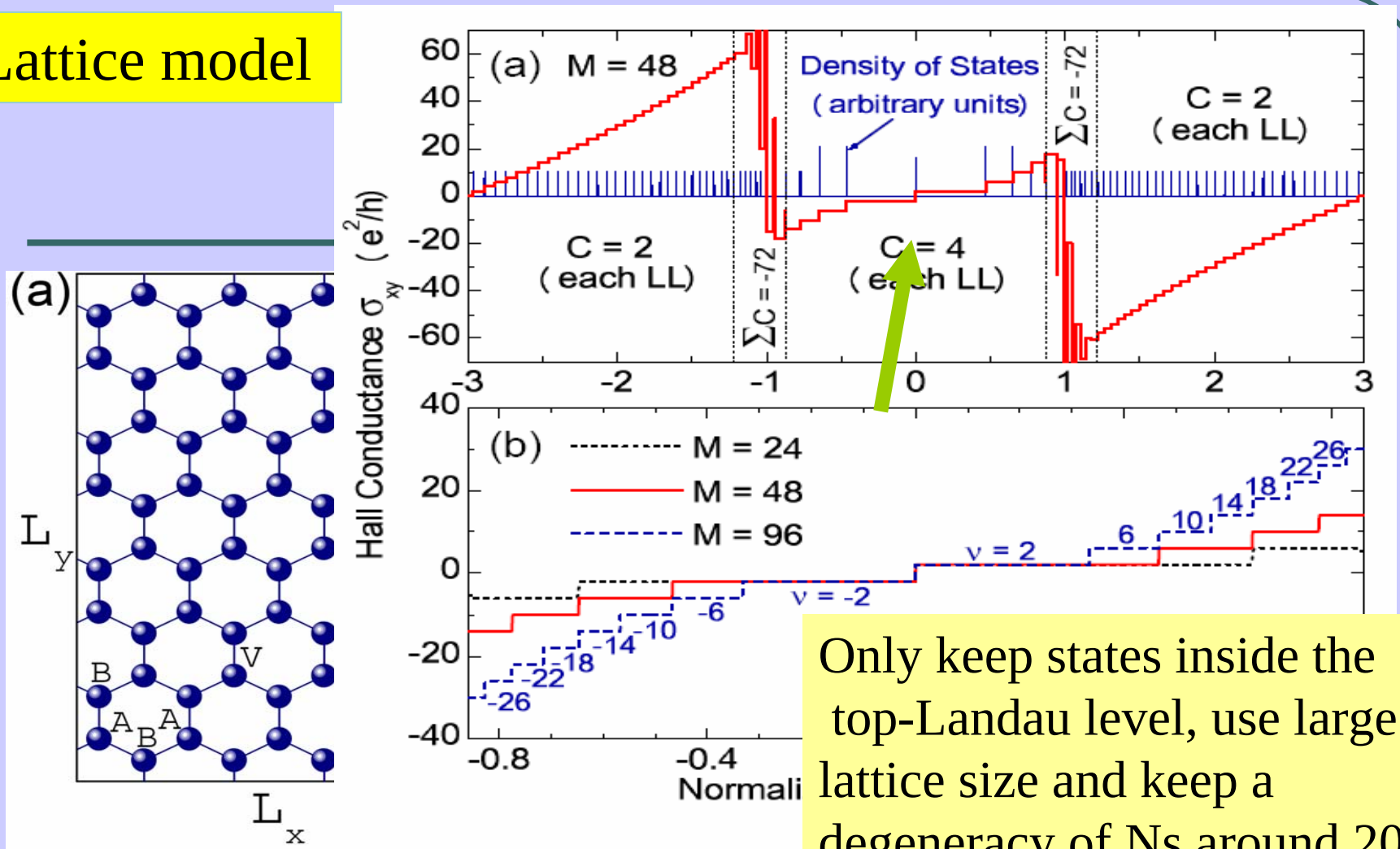

Only keep states inside the top-Landau level, use large lattice size and keep a degeneracy of Ns around 20 (assume real spin is polarized due to finite Zeeman energy)

$$H = -t\sum C_{iB}^{+} C_{jA} + h.c + \sum w_i C_i^{+} C_i$$

Energy spectrum for pure system

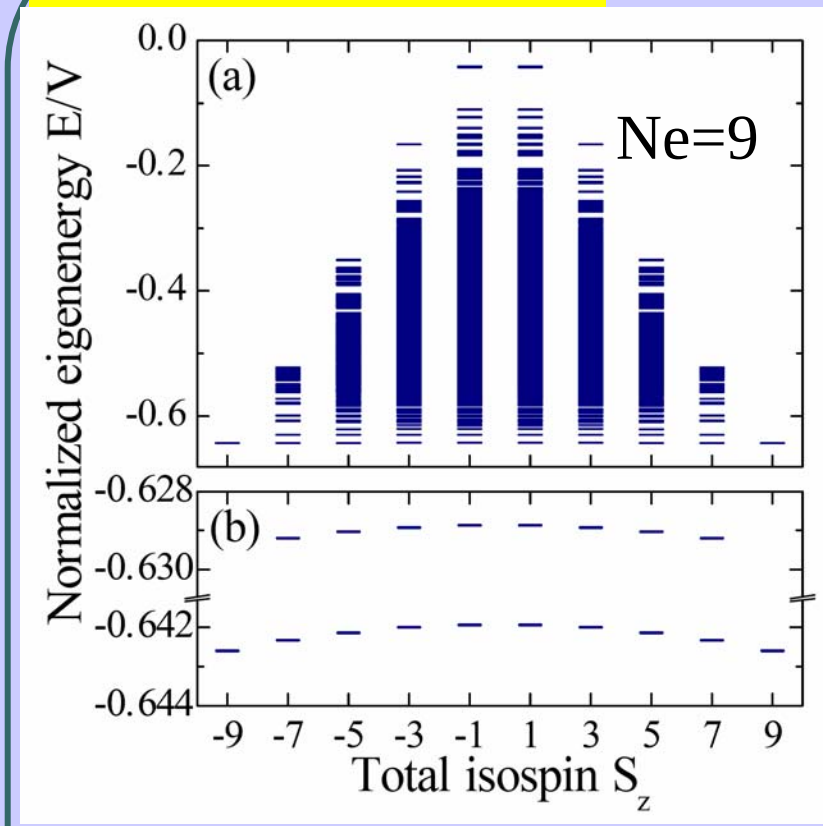

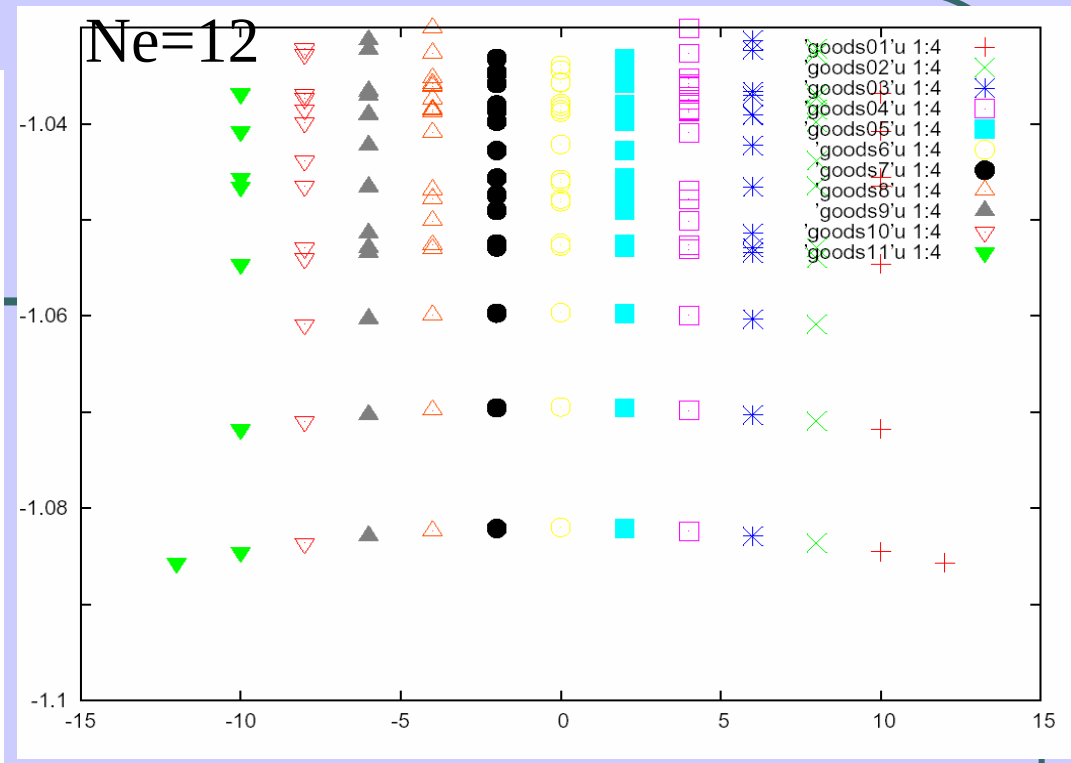

In each pseudo-spin sector, there is a FM state with "no double occupancy" and phase coherence

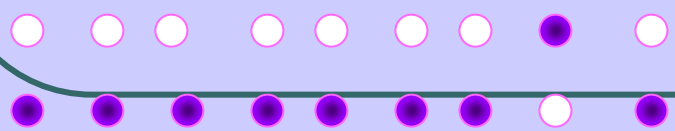

Anisotropic Energy

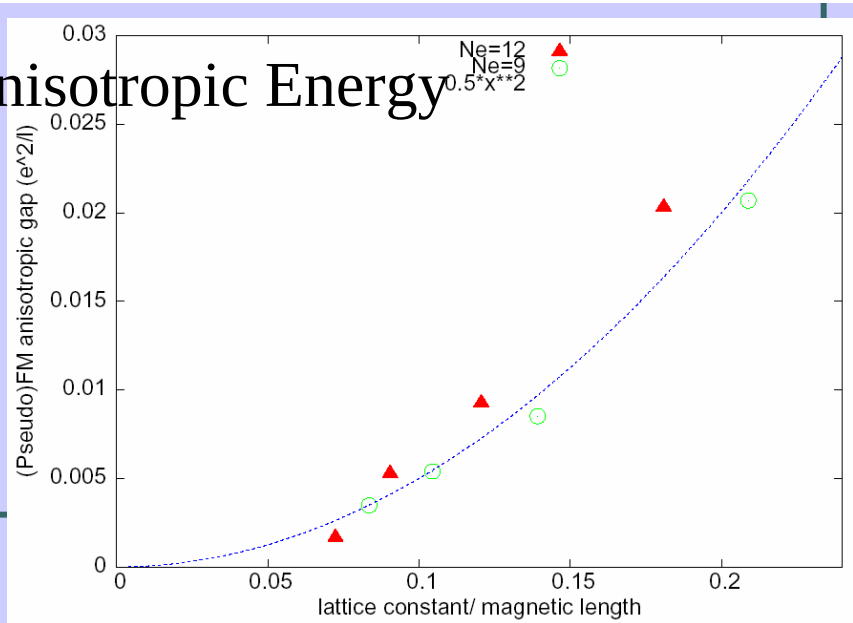

the excitation energy gap (with double occupation)

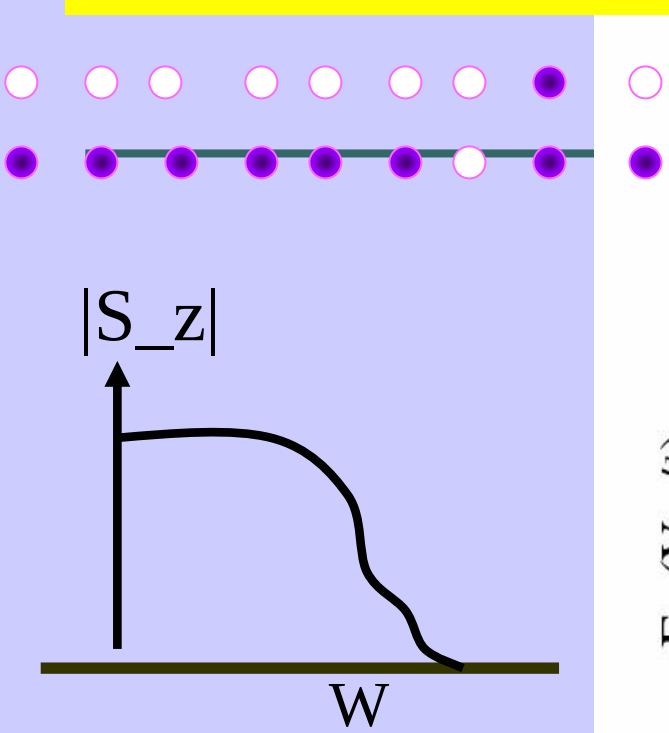

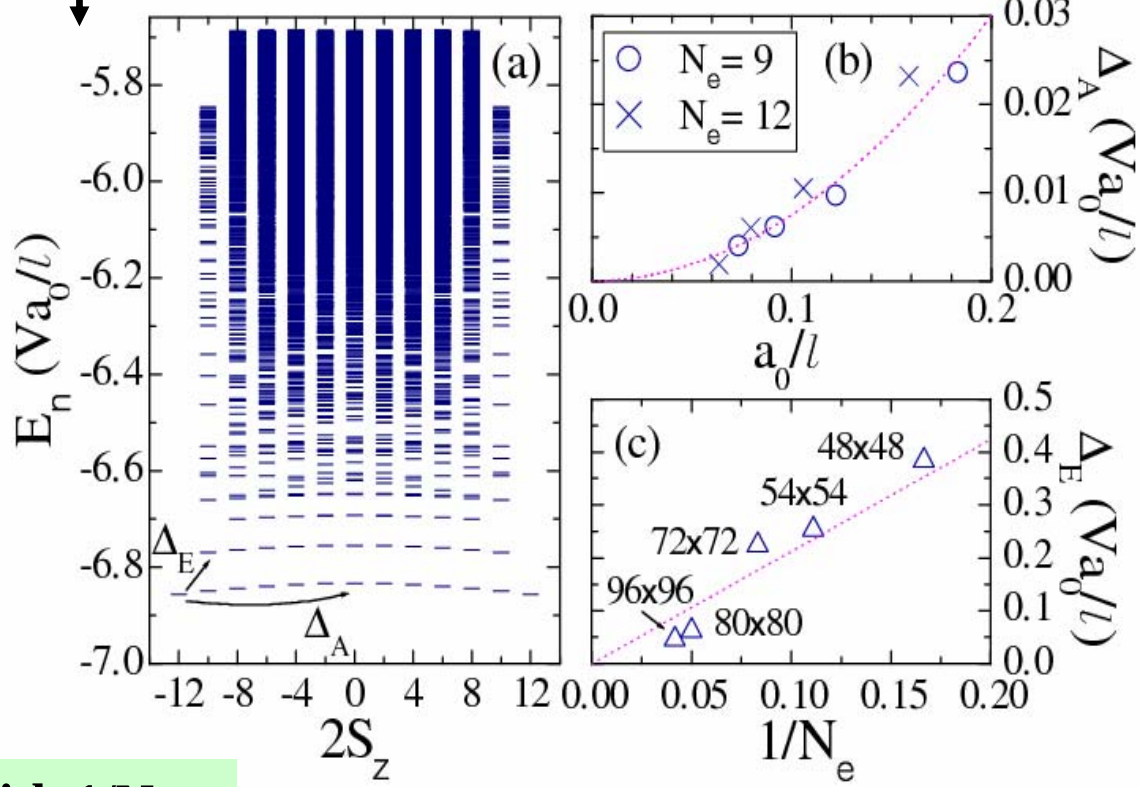

the excitation gap scales with 1/Ne, possibly extrapolates to zero at large Ne limit

Directly look at the transport property instead of “gaps”

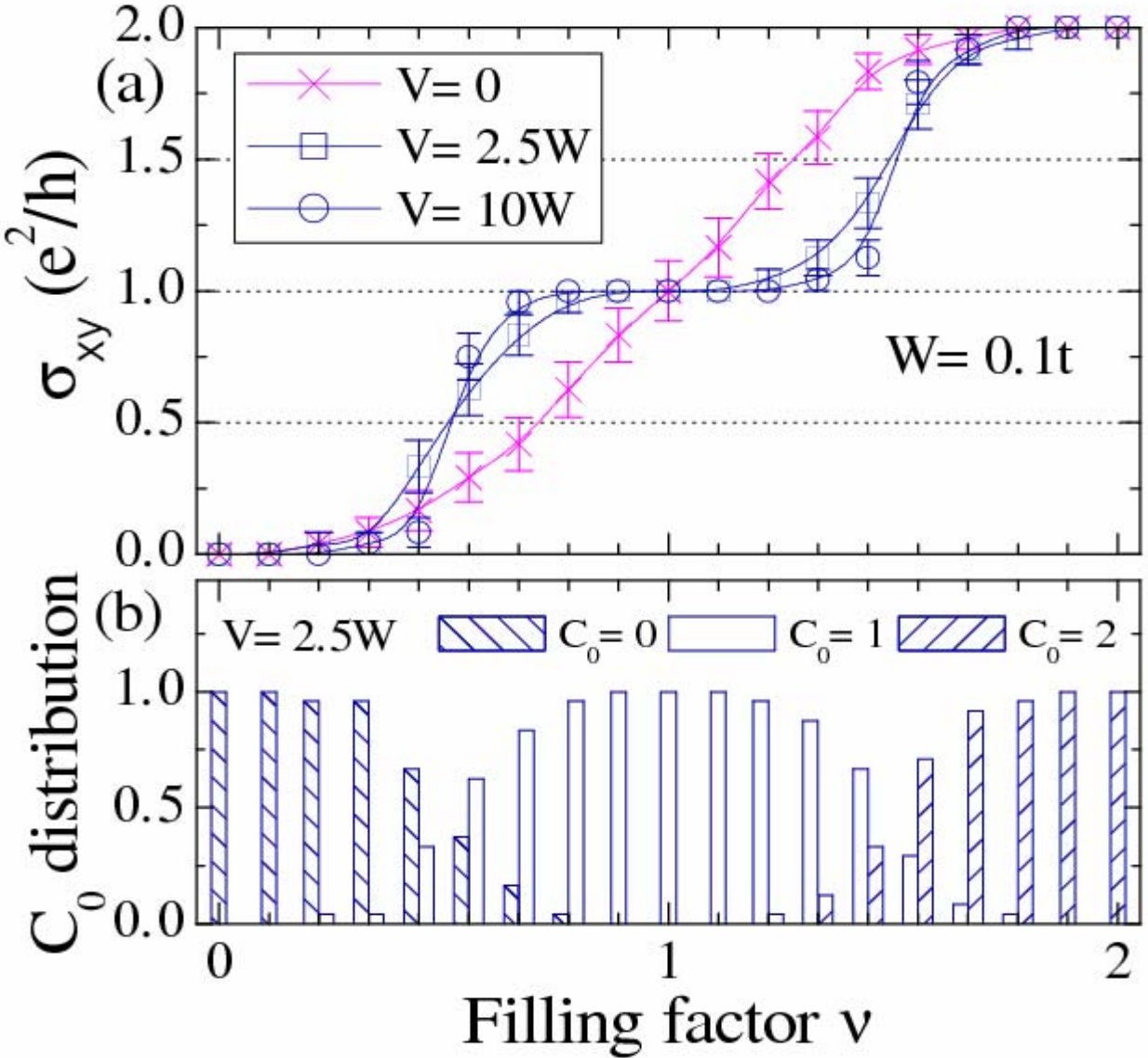

Chern number "IS" Hall conductance

D. J. Thouless et al 1982, J. E. Avron et al. 1883

$$\sigma_{xy} = \frac{ie^2h}{2\pi} \sum_{n>0} \frac{<0|p_x|n><n|p_y|0> - c.c}{(E_n - E_0)^2}$$

$$C = \frac{i}{4\pi} \oint d\theta_j \{\langle\psi|\frac{\partial\psi}{\partial\theta_j}\rangle - \langle\frac{\partial\psi}{\partial\theta_j}|\psi\rangle\} \qquad \sigma_{xy} = C\frac{e^2}{h}$$

$$C = \sum_{\varepsilon_m < \varepsilon_F} C^{(m)}$$

C is for many-body

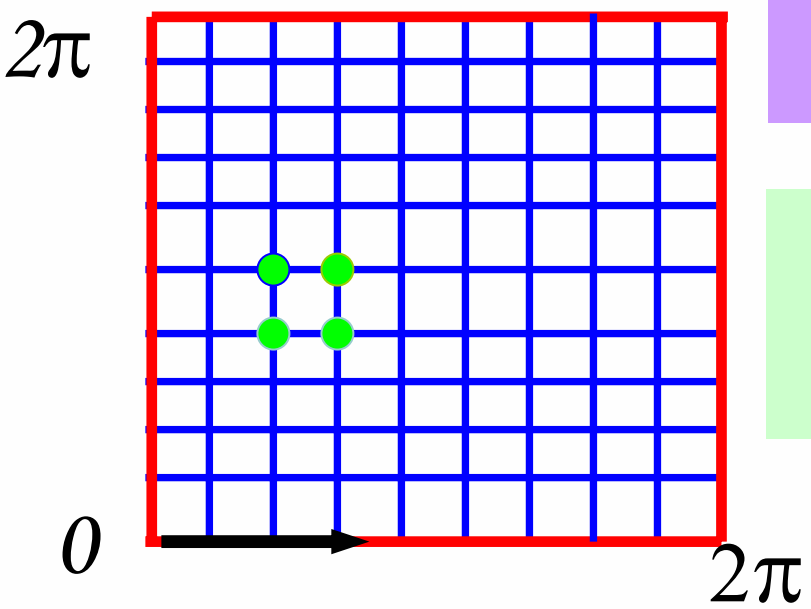

D.N. Sheng et al., PRL 2003;
Sheng, Balents, Wang
Xin et al. PRB (FQHE)

Just get ψ(θ) at all nodes of mesh of 100-1000 points, overlap of ψ(θ) at nearest points

The importance of mobility gap (activation gap of experiment): from direct Hall conductance and Chern number calculations

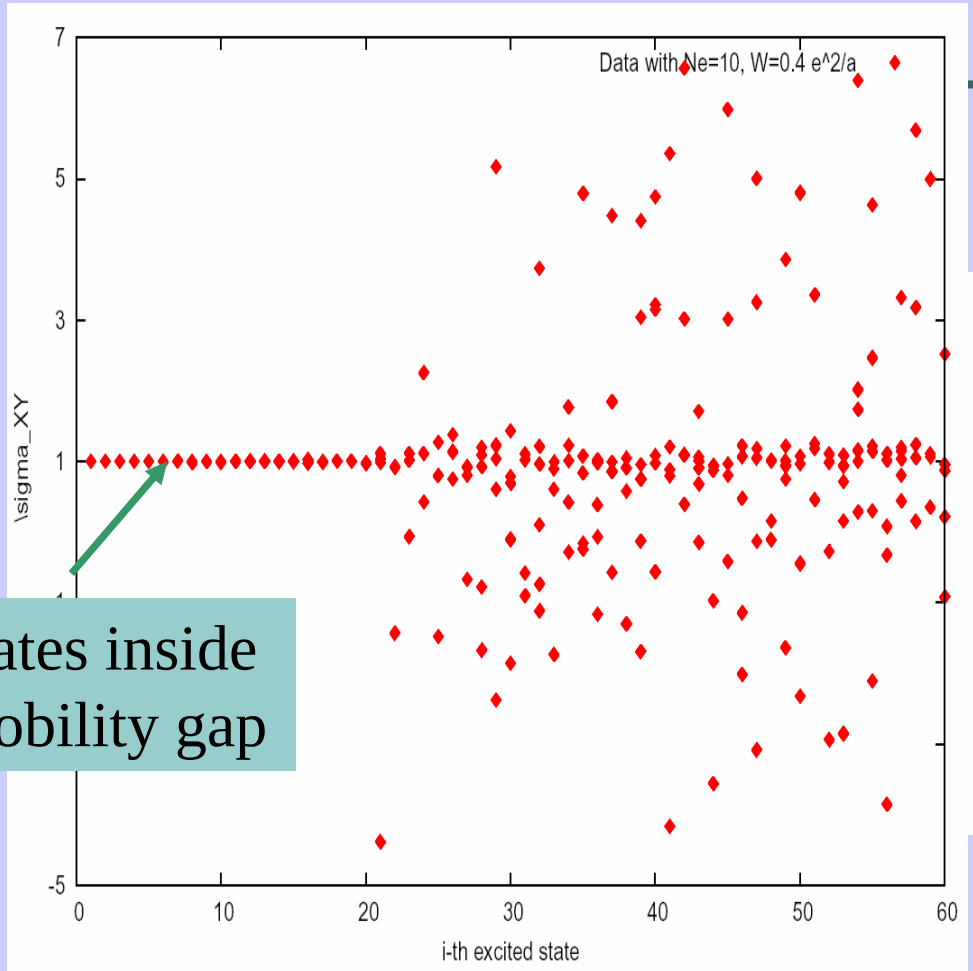

States inside mobility gap

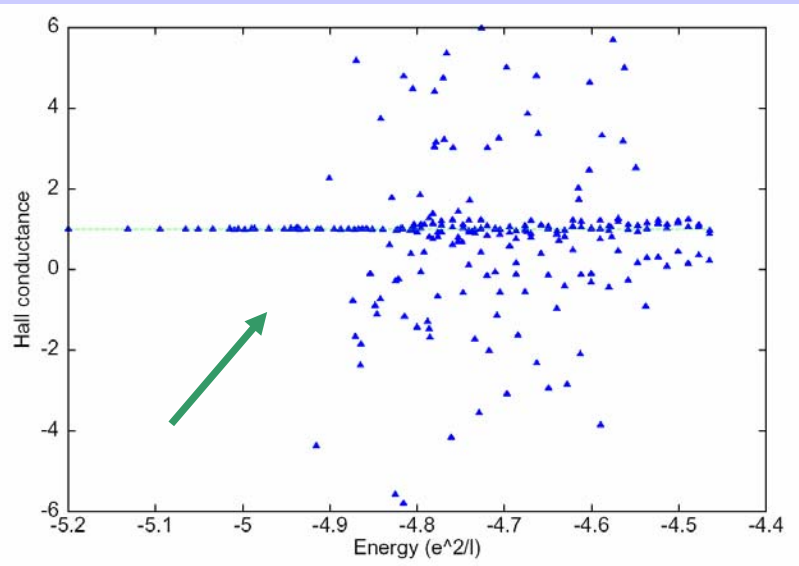

finite size scaling confirms a finite transport gap at large size limit (more data are coming)

Fluctuation of Chern numbers determine a mobility edge

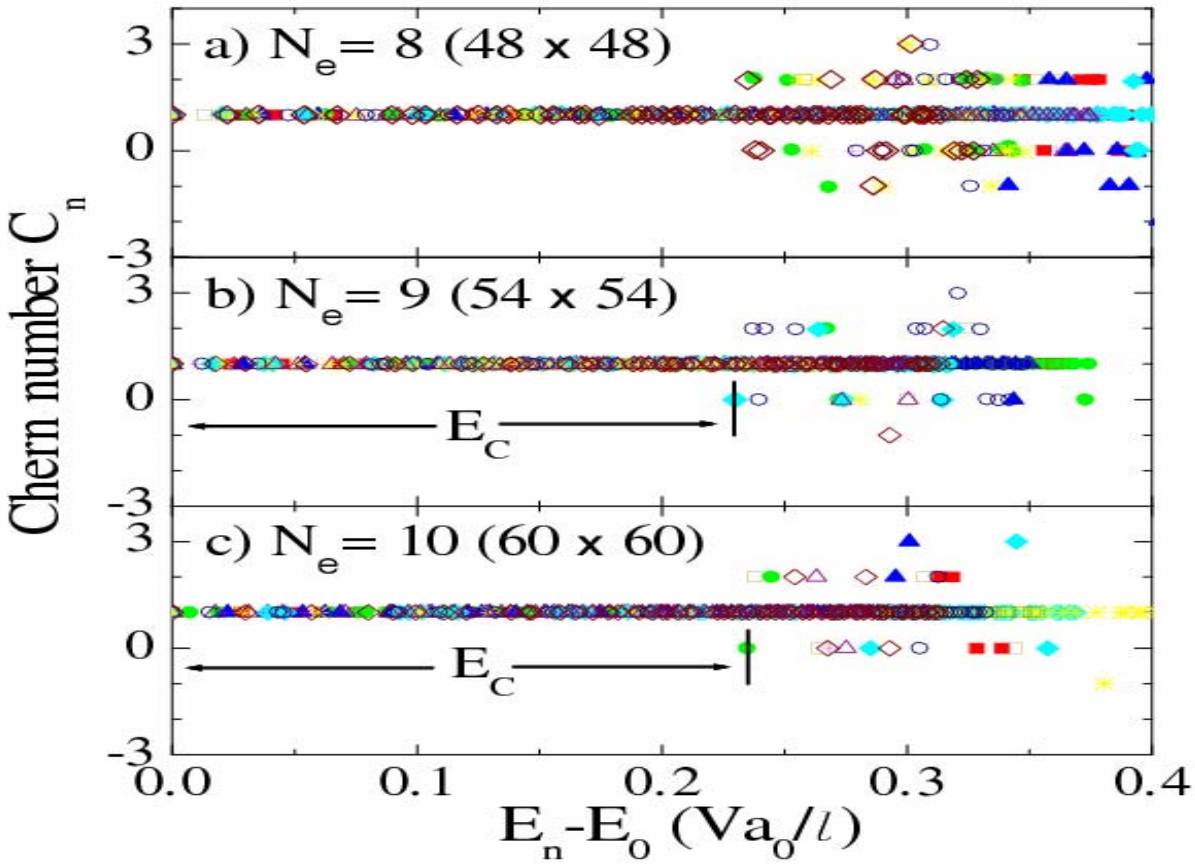

e^2/ εl

Mobility gaps

e^2/ ε l

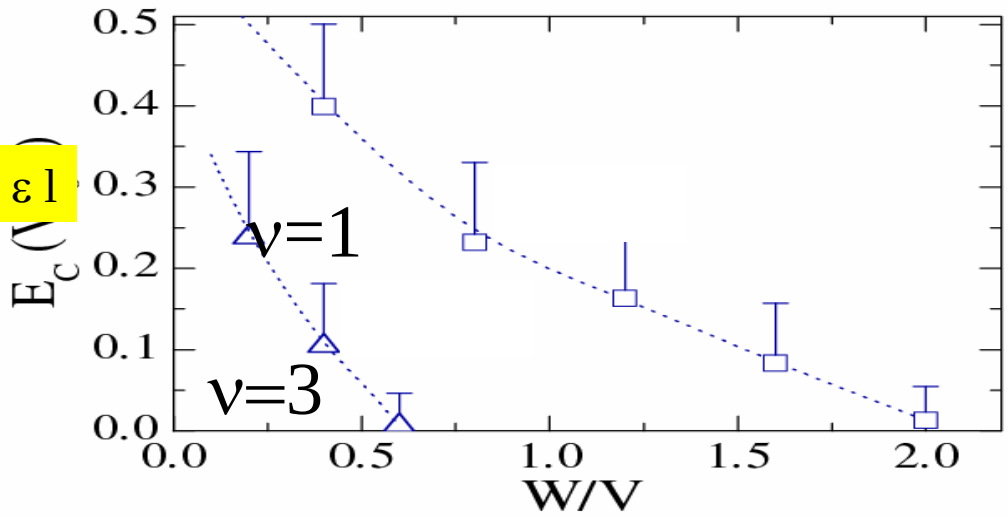

Summary:

The ν=1 IQHE is robust in both pseudo-spin FM state and pseudo-spin liquid like state, protected by a mobility gap (importance of localization in interacting system)

Quantitative results of activation (mobility) gap at different disorder strengths can be compared with experimental measurements

Topological order in SOC band insulator and SHE---honeycomb lattice model

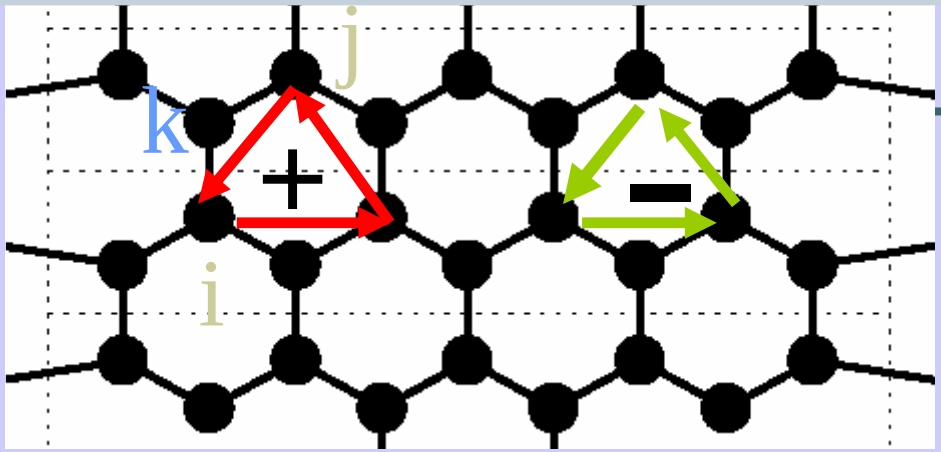

other models:
B. A. Bernevig and S. C. Zhang,
X. L. Qi, Y. S. Wu and S. C. Zhang
J. Moore, Sinitsyn et al, P. A. Lee

spin species, + & - IQHE

role of Rashba V_R

$$H = -t\sum_{\langle ij\rangle} c_i^\dagger c_j + \frac{2i}{\sqrt{3}}V_{\rm SO}\sum_{\langle\langle ij\rangle\rangle} c_i^\dagger \hat{\boldsymbol{\sigma}}\cdot(\mathbf{d}_{kj}\times\mathbf{d}_{ik})c_j$$

$$+ \; iV_{\rm R}\sum_{\langle ij\rangle} c_i^\dagger \hat{\mathbf{z}}\cdot(\hat{\boldsymbol{\sigma}}\times\mathbf{d}_{ij})c_j + \sum_i \epsilon_i c_i^\dagger c_i \;,$$

F. D. M. Haldane 1988, Kane and Mele 2004, 2005

L. Sheng, D. N. Sheng, C. S. Ting & F.D.M.Haldane 2005, 2006

LB formula

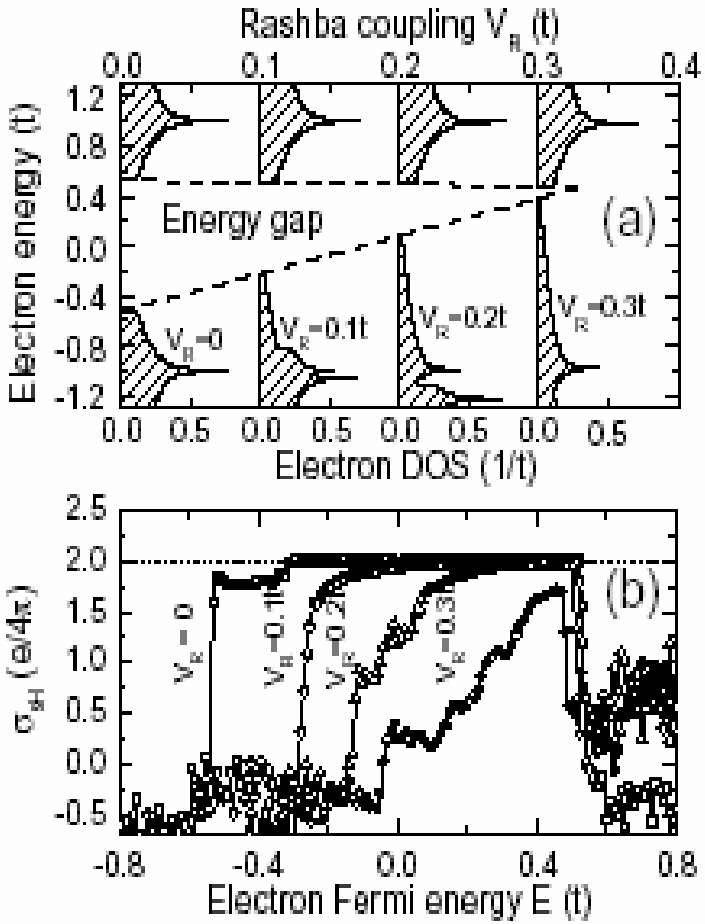
Rashba coupling V_R (t)
Electron energy (t)
Energy gap
(a)
V_R=0
V_R=0.1t
V_R=0.2t
V_R=0.3t
Electron DOS (1/t)
σ_{xH} (e/4π)
(b)
V_R = 0
V_R=0.1t
V_R=0.2t
V_R=0.3t
Electron Fermi energy E (t)

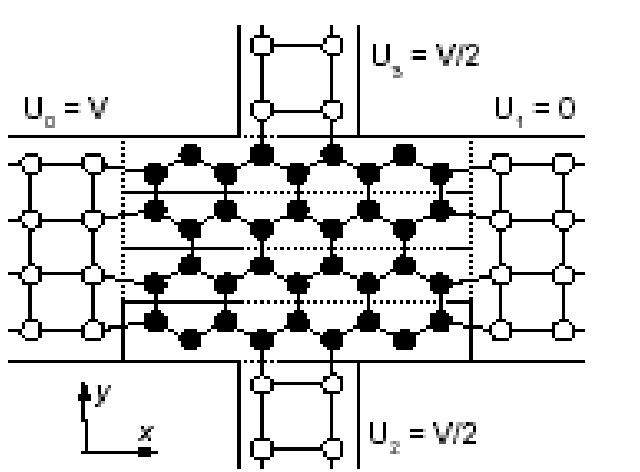
U_0 = V
U_1 = 0
U_2 = V/2
U_3 = V/2
y
x

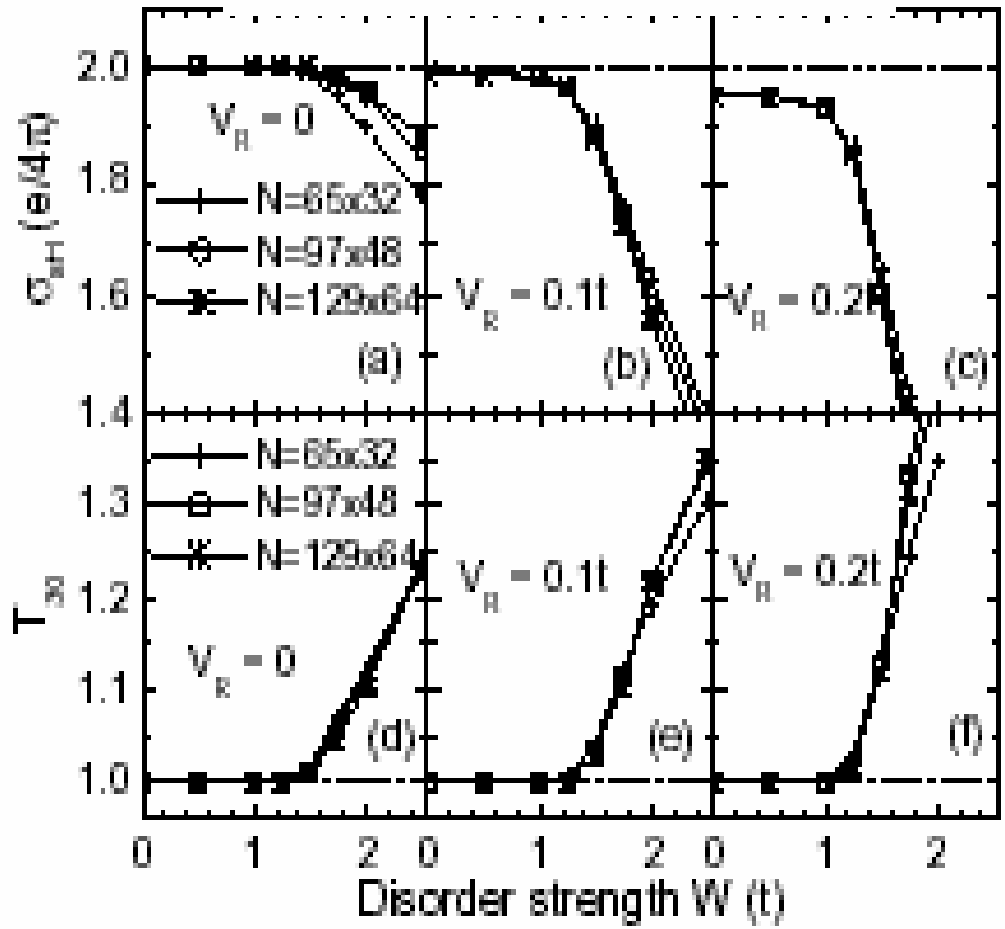
σ_{xH} (e/4π)
T_R
V_R = 0
N=65x32
N=97x48
N=129x64
(a)
V_R = 0.1t
(b)
V_R = 0.2t
(c)
V_R = 0
(d)
V_R = 0.1t
(e)
V_R = 0.2t
(f)
Disorder strength W (t)

Kubo formula for bulk SHC

$C^{SC} = C^{CS} = 2$

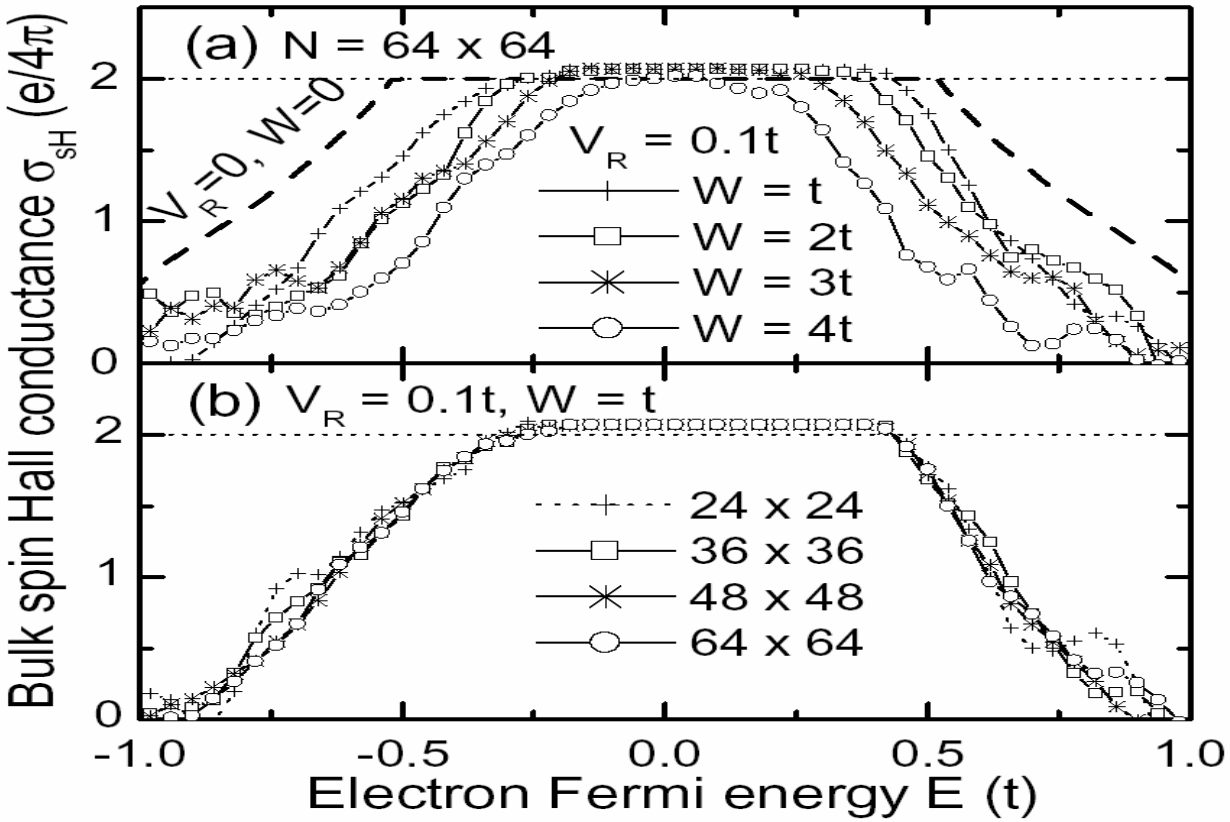

G. 4: Bulk SHC σ_{sH} calculated from the Kubo formula

robust and system size independent SHE only appears as $C^{SC} = C_1 - C_2 = 2$ phase, carried by two dissipationless edge states

Chern number

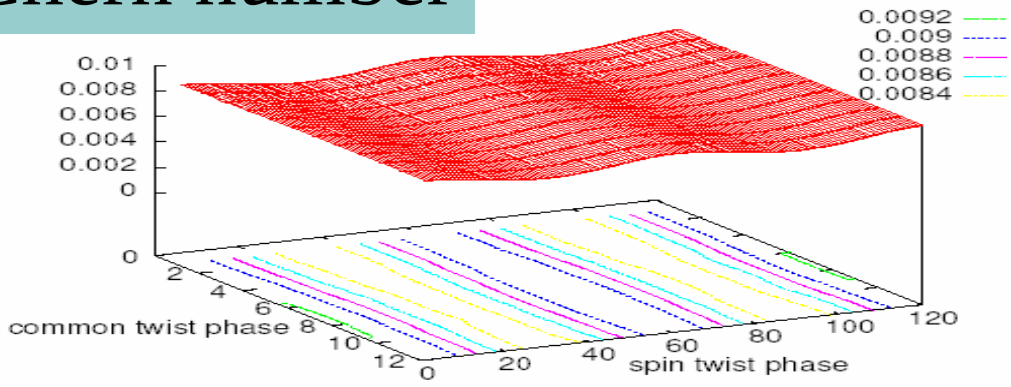

FIG. 1: Solid angle Ω_j as a function of two boundary phases (θ_x^s, θ_y^c), each θ unit cell is meshed into $N_{mesh} = 120 \times 12$ points for a pure system with $N_x = N_y = 60 \times 60$ at $V_{so} = 0.1$ and $V_R = 0.1$. Thus $\sum_{j=1}^{N_{mesh}} \Omega_j = 4\pi$, and $C_{sc} = 2$.

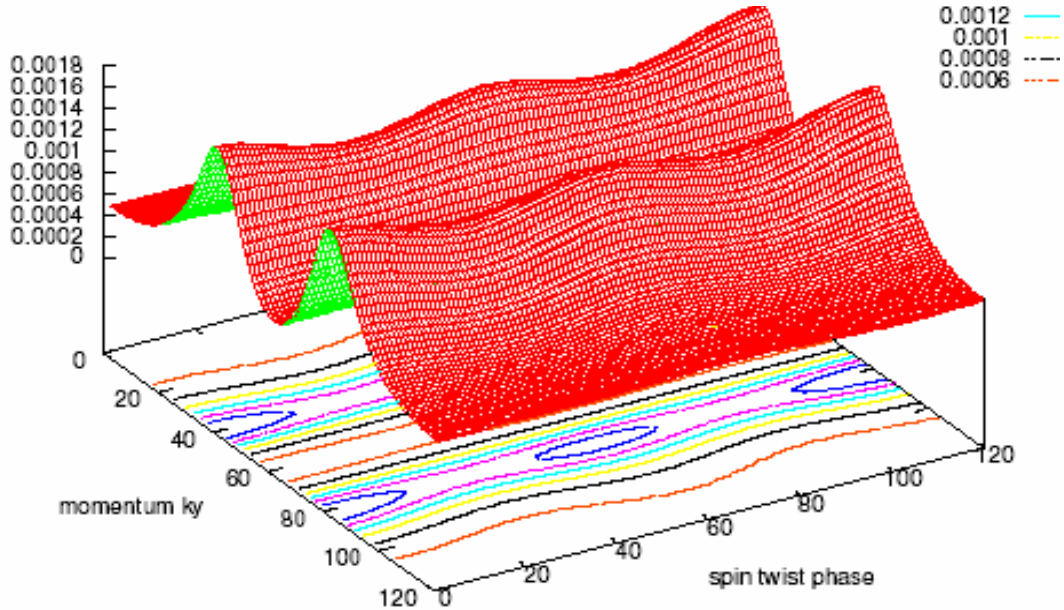

FIG. 2: Solid angle Ω_j as a function of spin twist and momentum k_y. Each $2\pi \times 2\pi$ unit cell is meshed into $N_{mesh} = 120 \times 120$ points for a pure system with $N_x = 60$ at $V_{so} = 0.1$ and $V_R = 0.1$. Thus $\sum_{j=1}^{N_{mesh}} \Omega_j = 4\pi$, and $C_{sc} = 2$.

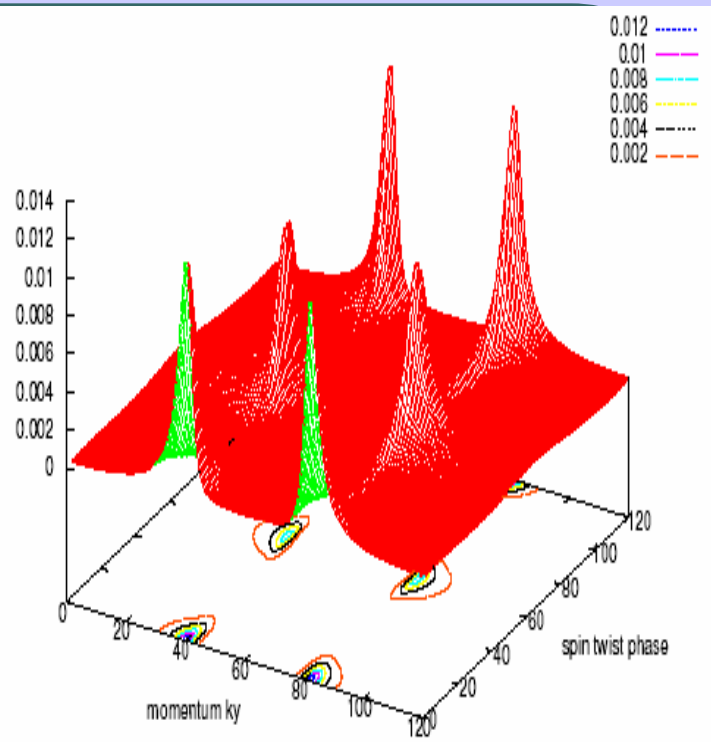

Spin polarization

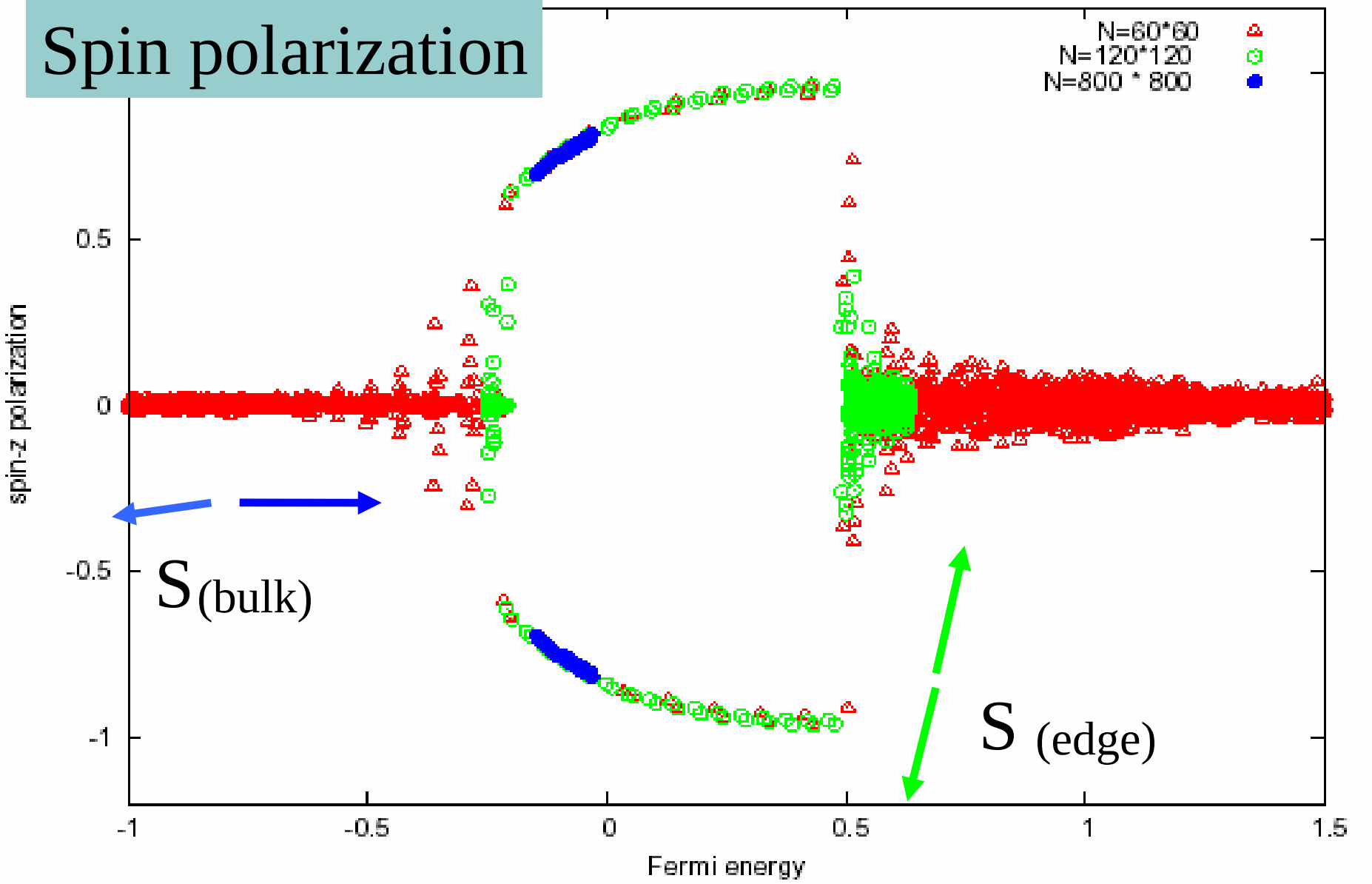

Spin 90% up state pumping to top, 90% down to bottom, SHC= 1.8 (e/4π)